

## Strongly Isolated Ferromagnetic Layers in Poly-*trans*- $\mu$ -dichloro- and Poly-*trans*- $\mu$ -dibromobis(1-(2-chloroethyl)-tetrazole-*N'*)copper(II) Complexes

Arno F. Stassen,<sup>†</sup> Huub Kooijman,<sup>‡</sup> Anthony L. Spek,<sup>‡</sup> L. Jos de Jongh,<sup>§</sup> Jaap G. Haasnoot,<sup>†,\*</sup> and Jan Reedijk<sup>†</sup>

Leiden Institute of Chemistry, Gorlaeus Laboratories, Leiden University, P.O. Box 9502, 2300 RA Leiden, The Netherlands, Bijvoet Center for Biomolecular Research, Crystal and Structural Chemistry, Utrecht University, Padualaan 8, 3584 CH Utrecht, The Netherlands, and Kamerlingh Onnes Laboratory, Leiden University, P.O. Box 9506, 2300 RA Leiden, The Netherlands

Received May 24, 2002

Two new isostructural compounds, dichlorobis(1-(2-chloroethyl)tetrazole)copper(II) (**1**) and dibromobis(1-(2-chloroethyl)tetrazole)copper(II) (**2**), have been prepared. The synthesis, characterization, and spectral and magnetic properties as well as the crystal and molecular structures of **1** and **2** have been studied. Both complexes form two-dimensional, distorted square grid planes of copper and halides, distinctly separated by layers of tetrazole ligands. The differential (ac) magnetic susceptibility,  $\chi = (\delta M/\delta H)_T$ , and magnetization  $M(H)$  of both complexes have been studied as a function of temperature and field. The compounds possess a ferromagnetic interaction within the isolated copper-halide layers ( $J/k_B = 8.0$  K,  $J/k_B = 10.2$  K, respectively, for the chloride and the bromide, and  $T_c = 4.75$  K,  $T_c = 8.01$  K). The magnetic coupling  $J/k_B$  between the different layers is found to be very weak ( $|J'/J| \leq 2 \times 10^{-2}$ ).

### Introduction

The combination of copper(II) salts with heterocyclic azole ligands leads to a tremendous diversity in structures. Copper(II) complexes are known from monomers<sup>1–4</sup> to polynuclear complexes<sup>4–8</sup> to polymers.<sup>9–11</sup> Only a few coordination

complexes of copper(II) are known in which square grids are present. In many of these complexes, one or more of the bridges are N,N'-didentate spacers. As a result, the Cu–Cu distances in these cases are rather large.<sup>12–17</sup> The presence of a coordination compound possessing a square grid of only copper and halide ions is even less common.<sup>11,18–23</sup>

\* To whom correspondence should be addressed. E-mail: haasnoot@chem.leidenuniv.nl.

<sup>†</sup> Leiden Institute of Chemistry, Gorlaeus Laboratories, Leiden University.

<sup>‡</sup> Utrecht University.

<sup>§</sup> Kamerlingh Onnes Laboratory, Leiden University.

- (1) Wijnands, P. E. M.; Wood, J. S.; Reedijk, J.; Maaskant, W. J. A. *Inorg. Chem.* **1996**, *35*, 1214–1222.
- (2) Ozarowski, A.; McGarvey, B. R. *Inorg. Chem.* **1989**, *28*, 2262–2266.
- (3) Pervukhina, N. V.; Podberezskaya, N. V.; Lavrenova, L. G. *J. Struct. Chem.* **1995**, *36*, 138–145.
- (4) Haasnoot, J. G. *Coord. Chem. Rev.* **2000**, *200*, 131–185.
- (5) Liu, J. C.; Song, Y.; Yu, Z.; Zhuang, J. Z.; Huang, X. Y.; You, X. Z. *Polyhedron* **1999**, *18*, 1491–1494.
- (6) Campbell, C. J.; Driessen, W. L.; Reedijk, J.; Smeets, W. J.; Spek, A. L. *J. Chem. Soc., Dalton Trans.* **1998**, *21*, 2703–2706.
- (7) Koolhaas, G. J. A. A.; Driessen, W. L.; Reedijk, J.; van der Plas, J. L.; de Graaff, R. A. G.; Gatteschi, D.; Kooijman, H.; Spek, A. L. *Inorg. Chem.* **1996**, *35*, 1509–1517.
- (8) Fu, D. G.; Chen, J.; Tan, X. S.; Li, J. J.; Zhang, S. W.; Zheng, P. J.; Tang, W. X. *Inorg. Chem.* **1997**, *36*, 220–225.
- (9) Garcia, Y.; van Koningsbruggen, P. J.; Bravic, G.; Guionneau, P.; Chasseau, A.; Cascarano, G. L.; Moscovici, J.; Lambert, K.; Michalowicz, A.; Kahn, O. *Inorg. Chem.* **1997**, *36*, 6357–6365.

- (10) Wu, L. P.; Yamagiwa, Y.; Kuroda-Sowa, T.; Kamikawa, T.; Munakata, M. *Inorg. Chem.* **1997**, 1555–1559.
- (11) Virovets, A. V.; Podberezskaya, N. V.; Lavrenova, L. G.; Bikzhanova, G. A. *Acta Crystallogr., Sect. C* **1995**, *6*, 1084–1087.
- (12) van Albada, G. A.; Guijt, R. C.; Haasnoot, J. G.; Lutz, M.; Spek, A. L.; Reedijk, J. *Eur. J. Inorg. Chem.* **2000**, *1*, 121–126.
- (13) Suenaga, Y.; Yan, S. G.; Wu, L. P.; Ino, I.; Kuroda-Sowa, T.; Maekawa, M.; Munakata, M. *J. Chem. Soc., Dalton Trans.* **1998**, *7*, 1121–1125.
- (14) Decurtins, S.; Schmalte, H. W.; Schneuwly, P.; Zheng, L. M.; Ensling, J.; Hauser, A. *Inorg. Chem.* **1995**, *34*, 5501–5506.
- (15) Kawata, S.; Breeze, S. R.; Wang, S. N.; Greedan, J. E.; Raju, N. P. *Chem. Commun.* **1997**, *7*, 717–718.
- (16) Tong, M. L.; Ye, B. H.; Cai, J. W.; Chen, X. M.; Ng, S. W. *Inorg. Chem.* **1998**, *37*, 2645–2650.
- (17) Engelfriet, D. W.; Groeneveld, W. L.; Nap, G. M. *Z. Naturforsch.* **1983**, *852*–864.
- (18) De Jongh, L. J.; Van Amstel, W. D.; Miedema, A. R. *Physica* **1972**, *58*, 277–304.
- (19) Lavrenova, L. G.; Bogatikov, A. N.; Ikorskii, V. N.; Sheludyakova, L. A.; Boguslavskii, E. G.; Gaponik, P. N.; Larionov, S. V. *Zh. Neorg. Khimii.* **1996**, *41*, 423–426.
- (20) Virovets, A. V.; Podberezskaya, N. V.; Lavrenova, L. G. *Polyhedron* **1994**, *13*, 2929–2932.

Previously, Virovets, Lavrenova, and co-workers reported the structures of [Cu(Rtz)<sub>2</sub>Cl<sub>2</sub>]<sub>n</sub> (Rtz = ethyltetrazole,<sup>11</sup> allyltetrazole,<sup>21</sup> and vinyltetrazole<sup>19</sup>) and the structure of *trans*-diaquabisdinitrato(1-phenyltetrazole)copper(II).<sup>20</sup> The crystal structures of the three chloride complexes are almost identical. The compounds crystallize in the *P*<sub>2</sub>/*c* space group and show a strong axial ligand effect. Two tetrazole ligands and four chlorides octahedrally surround the copper ion. The two tetrazole ligands and two of the chlorides lie in the equatorial plane of the copper. The axial chloride ligands result in longer Cu–Cl bond lengths. The copper and chloride ions form layers of distorted square grids. Layers of tetrazole ligands separate these copper/halide layers.

This paper deals with the first [Cu(1-alkyltetrazole)<sub>2</sub>X<sub>2</sub>]<sub>n</sub> complexes (with X = Cl or Br) of which both the structure and the magnetic properties are determined in detail. In both systems, the strongly isolated nature of the ferromagnetic layers is prominent.

## Experimental Section

**Physical Measurements.** Vis–NIR spectra were obtained on a Perkin-Elmer Lambda 900 spectrophotometer using the diffuse reflectance technique, with MgO as a reference. X-band powder EPR spectra were obtained on a JEOL RE2x electron spin resonance spectrometer using DPPH (*g* = 2.0036) as a standard. FTIR spectra were obtained on a Perkin-Elmer Paragon 1000 FTIR spectrophotometer equipped with a Golden Gate ATR device, using the diffuse reflectance technique (4000–300 cm<sup>−1</sup>, resolution 4 cm<sup>−1</sup>). Magnetism was measured in the temperature range 1.8–150 K versus a field of 100 G. Alternating current magnetic susceptibility was measured between 1.8 and 20 K at zero field and a frequency of 9 Hz. All magnetic measurements were performed on an MPMS-5 Quantum Design SQUID magnetometer. Data were corrected for magnetization of the sample holder and for diamagnetic contributions, which were estimated from the Pascal constants.<sup>24</sup> C, H, N determinations were performed on a Perkin-Elmer 2400 Series II analyzer.

**Synthesis.** All chemicals were commercially available and of sufficient purity. 1-(2-Chloroethyl)tetrazole (teec) has been obtained as described in the literature.<sup>25</sup>

**Synthesis of [Cu(teec)<sub>2</sub>Cl<sub>2</sub>]<sub>n</sub> (1).** The compound has been prepared by dissolving 1.0 mmol of CuCl<sub>2</sub> (0.134 g) and 2.0 mmol of teec (0.265 g) in 20 mL of hot ethanol. Green, plate-shaped crystals formed after 1 day in a yield of approximately 80%. Anal. Found (Calcd) for CuC<sub>6</sub>H<sub>10</sub>N<sub>8</sub>Cl<sub>4</sub>: C, 18.1 (18.0); H, 2.4 (2.5); N, 28.1 (28.0)%.

**Synthesis of [Cu(teec)<sub>2</sub>Br<sub>2</sub>]<sub>n</sub> (2).** The compound has been prepared by dissolving 1.0 mmol of CuBr<sub>2</sub> (0.223 g) and 2.0 mmol of teec (0.265 g) in 20 mL of hot ethanol. Yellow-brown, plate-shaped crystals formed after 1 day in a yield of approximately 80%. Anal. Found (Calcd) for CuC<sub>6</sub>H<sub>10</sub>N<sub>8</sub>Br<sub>2</sub>Cl<sub>2</sub>: C, 14.8 (14.8); H, 1.9 (2.1); N, 23.1 (22.9)%.

**Table 1.** Crystallographic Data for Compounds **1** and **2**, at 150 K

	<b>1</b>	<b>2</b>
formula	C <sub>6</sub> H <sub>10</sub> Cl <sub>4</sub> CuN <sub>8</sub>	C <sub>6</sub> H <sub>10</sub> Br <sub>2</sub> Cl <sub>2</sub> CuN <sub>8</sub>
MW	399.57	488.47
cryst syst	monoclinic	monoclinic
space group	<i>P</i> <sub>2</sub> / <i>c</i> (No. 14)	<i>P</i> <sub>2</sub> / <i>c</i> (No. 14)
<i>Z</i> (mononuclear units)	2	2
<i>a</i> , Å	13.883(2)	13.173(3)
<i>b</i> , Å	6.6819(12)	6.9196(12)
<i>c</i> , Å	7.2995(12)	7.6141(12)
<i>β</i> , deg	98.054(12)	91.491(10)
<i>V</i> , Å <sup>3</sup>	670.46(19)	693.8(2)
<i>D</i> <sub>calcd</sub> , g cm <sup>−3</sup>	1.9793(6)	2.3382(7)
<i>D</i> <sub>obsd</sub> , g cm <sup>−3</sup>	1.97	2.30
<i>μ</i> <sub>calcd</sub> , mm <sup>−1</sup> [Mo Kα]	2.423	7.716
<i>R</i> <sup>a</sup>	0.0238 [1534 <i>I</i> > 2σ( <i>I</i> )]	0.0185 [1472 <i>I</i> > 2σ( <i>I</i> )]
wR2 <sup>b</sup>	0.0680	0.0396
GO <sub>F</sub> on <i>F</i> <sup>2</sup> ( <i>S</i> )	1.104	1.085

$$^a R = \sum ||F_o| - |F_c|| / \sum |F_o|. \quad ^b wR2 = [\sum [w(F_o^2 - F_c^2)^2] / \sum [w(F_o^2)^2]]^{1/2}.$$

**Crystal Structure Determination.** Crystals suitable for X-ray structure determination were glued to the top of a glass capillary and transferred into the cold nitrogen stream on a Nonius Kappa CCD diffractometer on a rotating anode. Reduced-cell calculations did not indicate higher lattice symmetry.<sup>26</sup> Crystal data and details on data collection are presented in Table 1. Data were collected at 150 K using graphite-monochromated Mo Kα radiation (*λ* = 0.71073 Å). The structures were solved by automated direct methods using SHELXS86<sup>27</sup> and refined on *F*<sup>2</sup> using full-matrix least-squares techniques (SHELXL-97<sup>28</sup>). For both compounds, refinement converged with Δ/*σ*<sub>max</sub> ≤ 0.001 and Δ/*σ*<sub>av</sub> < 0.001. Hydrogen atoms were located on a difference Fourier map, and their coordinates were included as parameters on the refinement. Non-hydrogen atoms were refined with anisotropic displacement parameters. Hydrogen atoms were included in the refinement with a fixed isotropic atomic displacement parameter related to the value of the equivalent isotropic displacement parameter of their carrier atoms.

For **1**, 9949 reflections were measured (1.6° < *θ* < 27.50°, −18 < *h* < 18, −8 < *k* < 8, −7 < *l* < 9, *φ* and *ω* area detector scans, with a crystal to detector distance of 40 mm, 3.3 h X-ray exposure time), 1534 of which were unique (*R*<sub>int</sub> = 0.0539, *R*<sub>σ</sub> = 0.0246), using a blue-green crystal of approximate dimensions 0.1 × 0.3 × 0.3 mm<sup>3</sup>. An absorption correction based on multiple measurements of symmetry-related reflections was applied (PLATON/MULABS);<sup>29</sup> transmission range was 0.523–0.784. 108 parameters were refined; the final residual density was in the range −0.68 < Δ*ρ* < 0.52 e Å<sup>−3</sup>.

For **2**, 12909 reflections were measured (1.6° < *θ* < 27.50°, −16 < *h* < 17, −8 < *k* < 8, −9 < *l* < 9, *φ* and *ω* area detector scans, with a crystal to detector distance of 35 mm, 3.6 h X-ray exposure time), 1585 of which were unique (*R*<sub>int</sub> = 0.0363, *R*<sub>σ</sub> = 0.0250), using a gold-brown crystal of dimensions 0.008 × 0.150 × 0.350 mm<sup>3</sup>. An analytical absorption correction based on measured crystal dimensions was applied (PLATON/ABST),<sup>29</sup> transmission range 0.311–0.933. Parameters (108) were refined; the final residual density was in the range −0.42 < Δ*ρ* < 0.52 e Å<sup>−3</sup>.

Neutral atom scattering factors and anomalous dispersion corrections were taken from the International Tables for Crystal-

- (21) Virovets, A. V.; Baidina, I. A.; Alekseev, V. I.; Podberzskaya, N. V.; Lavrenova, L. G. *J. Struct. Chem.* **1996**, *37*, 288–294.  
 (22) de Jongh, L. J.; Botterman, A. C.; de Boer, F. R.; Miedema, A. R. *J. Appl. Phys.* **1969**, *40*, 1363–1365.  
 (23) Steijger, J. J. M.; Frikke, E.; de Jongh, L. J.; Huiskamp, W. *J. Physica* **1983**, *120B*, 202–205.  
 (24) Kolthoff, I. M.; Elving, P. J. *Treatise on Analytical Chemistry*; Wiley: New York, 1963; Vol. 4.  
 (25) Stassen, A. F.; Kooijman, H.; Spek, A. L.; Haasnoot, J. G.; Reedijk, J. *J. Chem. Cryst.* **2001**, 185–192.

- (26) Spek, A. L. *J. Appl. Crystallogr.* **1988**, *21*, 578–579.  
 (27) Sheldrick, G. M. *SHELXS-86 Program for crystal structure determination*; University of Göttingen: Göttingen, Germany, 1986.  
 (28) Sheldrick, G. M. *SHELXL-97. Program for crystal structure refinement*; University of Göttingen: Göttingen, Germany, 1997.  
 (29) de Meulenaer, J.; Tompa, H. *Acta Crystallogr.* **1965**, *19*, 1014–1018.

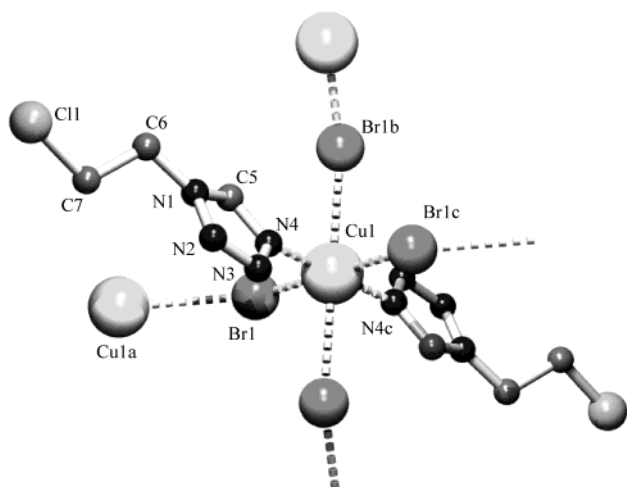


**Figure 1.** Basic molecular structure of  $[\text{Cu}(\text{teec})_2\text{Br}_2]_n$  (**2**) at 150 K, using Platon and POVray.<sup>31,39</sup>

**Table 2.** Relevant Bond Lengths in Compounds **1** and **2**

bond in <b>1</b>	distance (Å)	bond in <b>2</b>	distance (Å)
Cu(1)–Cl(1)	2.2948(5)	Br(1)–Cu(1)	2.4520(6)
Cl(1)–Cu(1)a	2.986(6)	Br(1)–Cu(1)a	3.0849(7)
Cu(1)–N(4)	1.9942(13)	Cu(1)–N(4)	1.9747(15)
Cu(1)–Cu(1)a	4.9480(9)	Cu(1)–Cu(1)a	5.1443(12)
N(1)–N(2)	1.354(2)	N(1)–N(2)	1.3529(18)
N(1)–C(5)	1.328(2)	N(1)–C(5)	1.328(3)
N(2)–N(3)	1.292(2)	N(2)–N(3)	1.290(2)
N(3)–N(4)	1.362(2)	N(3)–N(4)	1.3594(19)
N(4)–C(5)	1.3197(18)	N(4)–C(5)	1.314(3)

**Table 3.** Important Angles in Compounds **1** and **2**

<b>1</b>	angle (deg)	<b>2</b>	angle (deg)
Cu(1)–Cl(1)–Cu(1)b	138.70(2)	Cu(1)–Br(1)–Cu(1)a	136.29(1)
Cl(1)–Cu(1)–N(4)	90.58(4)	Br(1)–Cu(1)–N(4)	90.58(4)
Cl(1)–Cu(1)–Cl(1)a	92.32(2)	Br(1)–Cu(1)–Br(1)b	92.50(1)
N(4)–Cu(1)–Cl(1)a	88.31(4)	N(4)–Cu(1)–Br(1)b	90.04(4)

lography.<sup>30</sup> Geometrical calculations and illustrations were performed with PLATON.<sup>31</sup>

## Results

**Description of the Structures.** Both compounds **1** and **2** crystallize in molecular structures similar to previously reported  $[\text{Cu}(\text{alkyltetrazole})_2\text{Cl}_2]_n$  structures.<sup>11,18–21,23,32</sup> The exciting magnetic properties arise from their lattice arrangement described here. In both compounds, the coordination polyhedron of the Cu atom takes the form of an elongated square bipyramid with a  $-1$  symmetry (cf. Figure 1). The equatorial positions are occupied in **1** by two Cl atoms [ $\text{Cu}–\text{Cl} = 2.2948(5)$  Å] and the N4 atoms of the two planar teec ligands [ $\text{Cu}–\text{N} = 1.9942(13)$  Å] and in **2** by two bromide atoms [ $\text{Br}–\text{Cu} = 2.4520(6)$  Å] and the N4 atoms of the teec ligands [ $\text{Cu}–\text{N} = 1.9747(15)$  Å]. The axial positions are occupied in **1** by two chlorine atoms [ $\text{Cl}–\text{Cu} = 2.9864(6)$  Å] and in **2** by two bromide atoms [ $\text{Br}–\text{Cu} =$

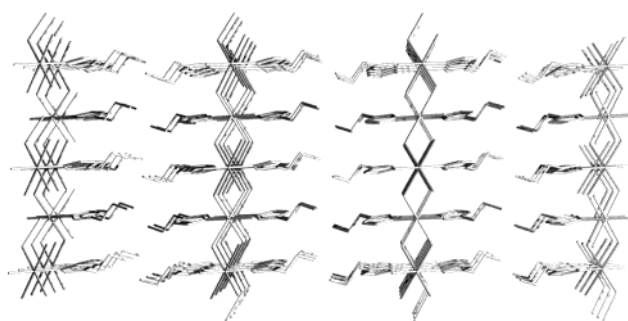


**Figure 2.** Platon projection of the presence of layers in compounds **1** and **2**.<sup>31,39</sup> The 2D plans are perpendicular to the projection planes.

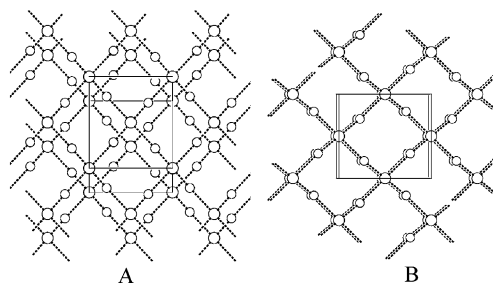


**Figure 3.** Parallel projection down the  $bc$ -plane on the copper–halide layers in **1** (A) and **2** (B).<sup>31</sup>

$3.0849(7)$  Å]. These axial halogen atoms are equatorial ligands for the neighboring molecules. Information concerning significant bond lengths is given in Table 2 for both complexes. Significant angles of the chloride and the bromide complexes are given in Table 3. Geometric characteristics of the tetrazole rings found in both complexes are in agreement with values found<sup>11,21</sup> for  $[\text{Cu}(\text{etz})_2\text{Cl}_2]$  and  $[\text{Cu}(\text{altz})_2\text{Cl}_2]$ . The two tetrazole rings lie in the same plane, as dictated by the  $-1$  symmetry.

In both complexes, the halide ions play the role of nonsymmetrical bridges and connect the molecules in infinite layers located in the  $bc$ -plane. The copper–halide layers are separated by the tetrazole ligands (cf. Figure 2). In **1**, the  $\text{Cu}–\text{Cl}–\text{Cu}$  angle is  $138.70(2)^\circ$ , while the  $\text{Cu}–\text{Cu}$  distance is  $4.9480(9)$  Å. In **2**, the  $\text{Cu}–\text{Br}–\text{Cu}$  angle is  $136.29(1)^\circ$  resulting in a  $\text{Cu}–\text{Cu}$  distance of  $5.1443(12)$  Å.

The distances between the different layers of copper and halide ions are  $13.746(2)$  Å in the chloride complex and  $13.169(3)$  Å in the bromide complex, equal to  $a \cdot \sin \beta$ . Although the two compounds are very similar in structure, they differ in the value of cell angle  $\beta$  ( $98^\circ$  in **1** versus  $91.5^\circ$  in **2**). This has an influence on both the distance between the copper layers and the projection parallel on the plane of the layers. In **2**, the grids lie almost on top of each other, with a shift of  $0.343$  Å between two layers (cf. Figure 3b). But in **1**, a much larger shift of  $1.945$  Å is visible (cf. Figure 3a).

The elongated axes lie in the  $bc$ -plane but are not all in the same direction. Half of them are along the  $\bar{b} + \bar{c}$  axis and half along the  $\bar{b} - \bar{c}$  axis (cf. Figure 4), resulting in orthogonal magnetic orbitals.

**Ligand Field and EPR Spectroscopy.** The ligand field spectrum has been measured in the diffuse reflection mode

(30) Wilson, A. J. C. *International Tables for Crystallography, Volume C*; Kluwer Academic Publishers: Dordrecht, The Netherlands, 1992.

(31) Spek, A. L. *PLATON, A multi-purpose crystallographic tool*; Spek, A. L., Ed.; Utrecht University: The Netherlands, 2001. Internet: <http://www.cryst.chem.uu.nl/platon>.

(32) Steijger, J. J. M.; Frikkee, E.; de Jongh, L. J.; Huiskamp, W. J. *Physica* **1984**, *123B*, 284–290.

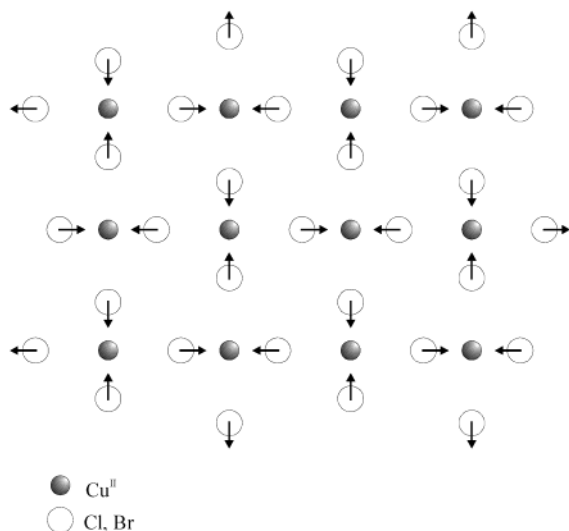


**Figure 4.** Basal plane (*bc*) in both complexes, with arrows indicating the shortest Jahn–Teller axis.<sup>35</sup>

**Table 4.** UV–Vis–NIR as Diffuse Reflection and EPR Spectra Data for Complexes **1** and **2**

compd	UV–vis–NIR ( $\text{cm}^{-1}$ )		EPR values, 77 K <sup>a</sup>				EPR value <sup>b</sup>
	$g_{\parallel}$	$g_{\perp}$	$A_{\parallel}$	$A_{NL}$	$A_{\perp}$	$g_{\perp}$	
<b>1</b>	$14.0 \times 10^3$	2.29	2.07	16.5	1.41	2.14	
<b>2</b>	$14.0 \times 10^3$	2.34	2.08	17.3		2.12	

<sup>a</sup> Spectra in frozen solution of MeOH. <sup>b</sup> Powder spectra at room temperature (broad band).

at room temperature. The d–d transitions in the UV–vis–NIR absorption spectra for both complexes are found at about  $1.4 \times 10^3 \text{ cm}^{-1}$  (cf. Table 4). These values agree with ligand field transitions for a square-based chromophore  $\text{CuN}_2\text{X}_4$ .<sup>33</sup> The  $g$  tensors obtained by EPR spectroscopy in frozen solution of MeOH are also listed in Table 4. Values found are in agreement with EPR values of  $\text{CuN}_2\text{X}_4$  compounds.<sup>34</sup>

**Magnetic Susceptibility.** In both compounds, two-dimensional grids are formed of  $\text{Cu}^{\text{II}}$  ions bridged by halide anions. A cooperative Jahn–Teller distortion occurs, as is common for  $\text{Cu}^{\text{II}}$  ions, with the result that the halogen ions are not positioned exactly between the two  $\text{Cu}^{\text{II}}$  ions but are displaced in such a way that the long axes of two nearest neighbor metal ions are mutually orthogonal (cf. Figure 4). The unpaired electron of each  $\text{Cu}^{\text{II}}$  occupies a d-type orbital pointing toward the two halogen ions and the two nitrogen atoms of the equatorial plane. These two halogen atoms are in the basal plane, while the nitrogen atoms are positioned on either side of the basal plane. Because of the cooperative Jahn–Teller ordering, the orbitals centered on adjacent metal ions are strictly orthogonal, and superexchange interactions within the plane are expected to be ferromagnetic.<sup>18,35</sup>

The magnetic susceptibility has been measured for both compounds between 2 and 150 K (cf. Figure 5; because magnetic properties of both compounds are very close, only

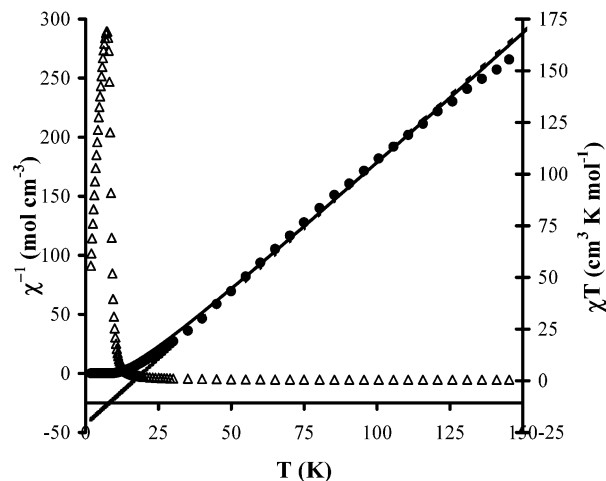


**Figure 5.**  $\chi^{-1}$  vs  $T$  ( $\bullet$ ) and  $\chi T$  vs  $T$  ( $\Delta$ ) of  $\text{Cu}(\text{teec})_2\text{Br}_2]_n$  (**2**) ( $\bullet$  = measured data, solid lines are the fits of the prediction for the two-dimensional Heisenberg  $S = 1/2$  ferromagnet from high-temperature series-expansion, dashed lines are the Curie–Weiss plots for clarity from near field theory).

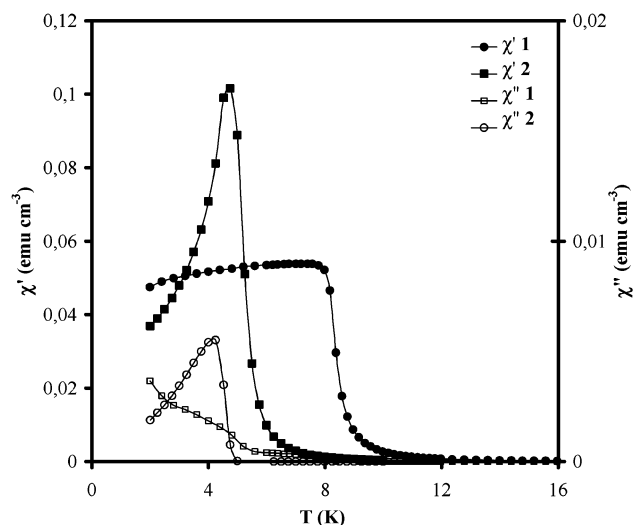


**Figure 6.** Real part ( $\chi'$ ) and imaginary part ( $\chi''$ ) of the susceptibility of the chloride and bromide complex against temperature.

the graph of **2** is plotted). As expected, because of the ferromagnetic interactions, deviations from the paramagnetic Curie–Weiss plots are observed at low temperature. The Curie constants  $C$  used for these plots are calculated from the  $g$  value obtained by EPR spectroscopy (cf. Table 4), with  $g_{\text{Cl}} = 2.14$  and  $g_{\text{Br}} = 2.17$ , with  $C_{\text{Cl}} = 0.43 \text{ cm}^3 \text{ K mol}^{-1}$  and  $C_{\text{Br}} = 0.45 \text{ cm}^3 \text{ K mol}^{-1}$ .<sup>36</sup>

Fitting of the linear part between 50 and 150 K results in Curie–Weiss temperatures of  $\theta_{\text{Cl}} = 15.0 \text{ K}$  and  $\theta_{\text{Br}} = 19.4 \text{ K}$ . Values for the actual transition temperatures  $T_c$  for the ferromagnetic ordering have been derived from zero-field ac susceptibility measurements (zero field, ac-frequency = 9.9 Hz) in which  $T_c$  is clearly indicated (cf. Figure 6).  $T_{c\text{Cl}} = 4.75 \text{ K}$ , where  $T_{c\text{Br}}$  is 8.01 K. These  $T_c$  values are lower than those of comparable structures found by De Jongh et al.,<sup>37</sup> but also in those systems, the  $T_c$  of the bromide is higher

(33) Hathaway, B. J.; Billings, D. E. *Coord. Chem. Rev.* **1970**, *5*, 143–207.

(34) van Albada, G. A.; Smeets, W. J. J.; Veldman, N.; Spek, A. L.; Reedijk, J. *Inorg. Chim. Acta* **1999**, 105–112.

(35) Kahn, O. *Molecular magnetism*; Wiley-VCH: New York, 1993.

(36) Carlin, R. L. *Magneto Chemistry*; Springer-Verlag: Berlin, 1986.

(37) De Jongh, L. J.; Miedema, A. R. *Adv. Phys.* **1974**, *23*, 1–265; **2001**, *50*, 947–1170.

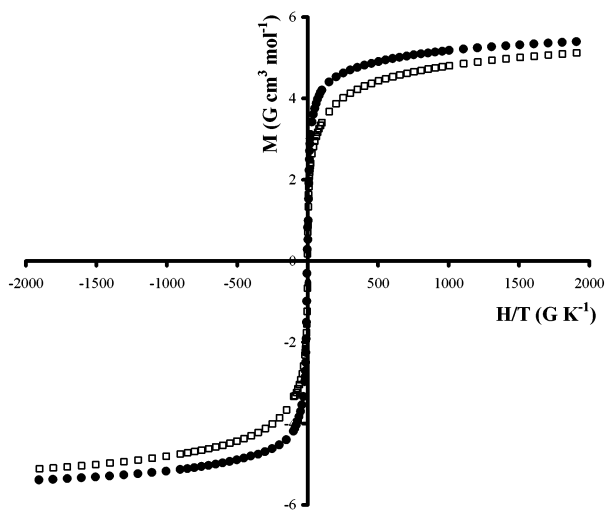


**Figure 7.** Magnetization at 5 K of  $[\text{Cu}(\text{teec})_2\text{Cl}_2]_n$  (**1**) ( $\square$ ) and  $[\text{Cu}(\text{teec})_2\text{Br}_2]_n$  (**2**) ( $\bullet$ ).

than that of the chloride. The fact that the  $T_c$  values are much lower than the Curie–Weiss temperatures  $\theta$  can be ascribed to the pronounced two-dimensional character of these materials. Because sufficiently large single crystals are not available, all measurements have been performed on polycrystalline samples. Therefore, no distinction can be made between the different crystal axes. A sharp maximum is visible in the graph of  $\chi'_{\text{Cl}}$ , whereas the graph of  $\chi'_{\text{Br}}$  shows a more gentle slope at temperatures below  $T_c$ .

Variable-field measurements at constant temperature (5 K) show that both compounds behave as almost ideal soft ferromagnets (cf. Figure 7), because no hysteresis effect is observed. A maximum magnetization of  $M_{S(\text{Cl})} = 5.46 \text{ G cm}^3 \text{ mol}^{-1}$  is observed for the chloride compound and for the bromide compound of  $M_{S(\text{Br})} = 5.73 \text{ G cm}^3 \text{ mol}^{-1}$  at 5 K. Both values are lower than the theoretical value of  $M_S (=N\mu_B g S) = \sim 6.0 \text{ G cm}^3 \text{ mol}^{-1}$ . This high value would only be reached at very high fields. From the more gradual slope of **1**, it can be seen that the measurement has been conducted above  $T_c$ .

The demagnetization factor  $D$  is calculated by determining the slope of the linear part of the magnetization curve.<sup>37</sup> This slope is equal to  $1/D$ .  $D$  is therefore an indicator of how close the behavior of the measured compound is to an “ideal” ferromagnet (for an ideal ferromagnet  $D = 0$ ). In a ferromagnet with small anisotropy, the powder susceptibility at  $T_c$  is expected to reach values close to the limit  $1/D \cdot \rho$ , as calculated for an ideal, isotropic ferromagnetic sample. Here,  $D/4\pi$  is the demagnetizing factor appropriate to the sample dimensions, and  $\rho$  is the density of the sample. For a powder,  $\rho$  will be somewhat lower (i.e., 30–40%) than the bulk value for a crystalline sample. Furthermore, accurate values for the (effective) demagnetizing factor in a powder are difficult to obtain, so one may set tentatively  $D/4\pi$  equal to one-third, as appropriate for a spherical crystal. This leads to the rough estimate  $1/D \cdot \rho \sim 0.15 \text{ cm}^3 \text{ g}$ . The experimental values reached at  $T_c$  (cf. Figure 6) are required to be of this order of magnitude, taking into account the mentioned uncertainties and the fact that the experimental powder susceptibilities will

be lowered because of the anisotropy. This analysis, combined with the shape of the magnetization curves in Figure 7, provides compelling evidence for the fact that the magnetic ordering is indeed ferromagnetic.

## Discussion and Conclusion

The compounds dichlorobis(1-(2-chloroethyl)tetrazole)-copper(II) and dibromobis(1-(2-chloroethyl)tetrazole)copper(II) crystallize in the  $P2_1/c$  space group with similar cell dimensions and structure. The structure can be seen as two-dimensional planes of square grids, with copper ions on the corners and halide ions in the middle of the sides. The planes are separated by layers of neutral ligands, which only have van der Waals contacts. No indication of covalent or hydrogen bonding, or stacking, is seen between the teec layers.

The elongated axes of the  $\text{Cu}^{\text{II}}$  ion lie in the copper–halide planes. Half of these elongated axes lie along the  $\vec{b} + \vec{c}$  axis and half along the  $\vec{b} - \vec{c}$ . This results in a soft ferromagnetic coupling. This coupling has also been observed in the structurally related compounds<sup>37</sup> with general formula  $[(\text{C}_n\text{H}_{2n+1}\text{NH}_3)_2\text{CuX}_4]_n$  with  $\text{X} = \text{Cl}, \text{Br}$ .

Values for the exchange parameter  $J/k_B$  have been obtained by fitting the data above  $T_c$  (between approximately 20 and 250 K) to an expression for the susceptibility derived from high-temperature series expansion results for the isotropic ferromagnetic quadratic lattice with spin  $S = 1/2$ . The results of Baker et al.<sup>38</sup> for the two-dimensional Heisenberg model have been used to fit the data. The series takes the following form:

$$\chi = \left(\frac{C}{T}\right) \cdot \left[1 + \sum_{n \geq 1} \frac{\alpha_n}{2^n n!} x^n\right]$$

with  $n =$  integer values from 1 to 10,  $x = J/k_B T$ , and  $\alpha_n$  the coefficient for the square lattice. For  $S = 1/2$ , the  $\alpha_n$  values are known up to  $n = 10$ . Using the Curie constants, calculated from the EPR data for the  $\mathbf{g}$  tensors, the interlayer exchange parameters of both compounds are found to be  $J_{\text{Cl}}/k_B = 8.0 \text{ K}$  and  $J_{\text{Br}}/k_B = 10.2 \text{ K}$ . When considering that the Curie–Weiss temperature  $\theta$  is equal to  $2J/k_B$ , the values of  $J/k_B$  obtained from the Curie–Weiss temperatures cited here are  $J_{\text{Cl}}/k_B = 7.5 \text{ K}$ ,  $J_{\text{Br}}/k_B = 9.7 \text{ K}$ . These values are in agreement with the values obtained from the fit to the two-dimensional Heisenberg model.

The value of  $k_B T_c/J$  can be regarded as an indication for the smallness of the ratio of the interlayer exchange parameter  $J'/k_B$  and the intralayer exchange parameter.<sup>37</sup> For the chloride,  $k_B T_{c\text{Cl}}/J_{\text{Cl}} = 0.56$ , whereas for the bromide complex,  $k_B T_{c\text{Br}}/J_{\text{Br}} = 0.79$ . The value for the chloride compound is close to that<sup>37</sup> found for  $[(\text{C}_2\text{H}_5\text{NH}_3)_2\text{CuCl}_4]_n$ , with  $k_B T_c/J = 0.55$ . For this compound, a ratio  $|J'/J| \sim 8.5 \times 10^{-4}$  was found. The value found for the bromide compound is higher than reported for the comparable bis-

(38) Baker, G. A.; Gilbert, H. E.; Eve, J.; Rushbrooke, G. S. *Phys. Lett.* **1967**, 25A, 207–209.

(39) Carson, C. *POVRAY, rendering engine for Windows*; 1996–1999.

(alkylamino)copper(II) bromide compound<sup>37</sup> and is closer to those for Rb<sub>2</sub>CuCl<sub>4</sub> and Rb<sub>2</sub>CuCl<sub>3</sub>Br (respectively, 0.73 and 0.86).<sup>37</sup> This lattice comparison would give an estimated value of  $|J'_{\text{Br}}/J_{\text{Br}}| \sim 1 \times 10^{-2}$  for the bromide compound. From these comparisons, it can be concluded that the interlayer exchange coupling  $J'$  is in both compounds several orders smaller than the intralayer exchange coupling  $J$ . These compounds can therefore indeed be considered as being organized of almost fully isolated two-dimensional ferromagnetic layers.

**Acknowledgment.** The work described in the present paper has been supported by the Leiden University Study group WFMO. We acknowledge financial support by the

European Union, allowing regular exchange of preliminary results with several European colleagues in the TOSS network, under Contract ERB-FMNRX-CT98-0199. Support by the ESF Programme Molecular Magnets (1998–2003) is kindly acknowledged. This work was also financially supported in part (A.L.S.) by the Council for the Chemical Sciences of The Netherlands Organization for Scientific Research (CW-NWO).

**Supporting Information Available:** Crystallographic data in CIF format. This material is available free of charge via the Internet at <http://pubs.acs.org>.

IC0257470